Investigating the Effect of NO on the Capture of CO_2 using Superbase Ionic Liquids for Flue Gas Applications

Adam J. Greer[†,‡,], S. F. Rebecca Taylor[‡], Helen Daly[‡], Matthew Quesne[#], Richard Catlow[#], Johan Jacquemin[†,§,*], Christopher Hardacre[‡,*]*

[†]School of Chemistry and Chemical Engineering, Queen's University Belfast, David Keir Building, Stranmillis Road, Belfast, BT9 5AG, Northern Ireland

[‡]School of Chemical Engineering and Analytical Science, The University of Manchester, The Mill, Sackville Street, Manchester, M13 9PL, United Kingdom

[#]School of Chemistry, Cardiff University, Main Building, Park Place, Cardiff, CF10 3AT, United Kingdom

[§]Université de Tours, Laboratoire PCM2E, Parc de Grandmont, Avenue Monge, 37200, Tours, France

AUTHOR INFORMATION

Co-Corresponding Authors:

* Christopher Hardacre, School of Chemical Engineering and Analytical Science, The University of Manchester, The Mill, Sackville Street, Manchester, M13 9PL, United Kingdom. Tel: +44 (0) 161 3062672, E-mail: c.hardacre@manchester.ac.uk

* Johan Jacquemin, Université de Tours, Laboratoire PCM2E, Parc de Grandmont, Avenue Monge, 37200, Tours, France. Tel: +33 (0) 2 47 36 73 29, Fax: +33 (0) 2 47 36 70 73, E-mail: jj@univ-tours.fr

* Adam Greer, School of Chemical Engineering and Analytical Science, The University of Manchester, The Mill, Sackville Street, Manchester, M13 9PL, United Kingdom. Tel: +44 (0) 161 3062227, E-mail: adam.greer@manchester.ac.uk

Abstract

The effect of acidic gases present in flue gas, specifically NO, on the capture of CO_2 by the superbase ionic liquid, trihexyltetradecylphosphonium benzimidazolide ([P_{66614}][Benzim]), is reported. An online mass spectrometry technique was utilized to study the CO_2 uptake of the ionic liquid during multiple absorption and desorption cycles of a gas feed containing NO and CO_2 at realistic flue gas concentrations, and it was found that while NO alone could bind irreversibly, the CO_2 capacity of the IL was largely unaffected by the presence of NO in a co-feed of the gases. *In-situ* attenuated total reflection (ATR) infrared was employed to probe the competitive absorption of CO_2 and NO by [P_{66614}][Benzim], in which carbamate and NONOate species were observed to co-bind to different sites of the benzimidazolide anion. These effects were further characterised by analysing changes in physical properties (viscosity and nitrogen content) and other spectroscopic changes (^{1}H NMR, ^{13}C NMR and XPS). Density functional theory (DFT) computations were used to calculate binding energies and infrared frequencies of the absorption products, which were shown to corroborate the results and explain the reaction pathways.

Keywords: Ionic Liquids; Flue Gas; Competitive Absorption; CO_2 Capture; NO; Infrared; DFT

Introduction

Ionic liquids (ILs) have been shown to be suitable for a wide range of applications because of their physical properties, such as a high thermal stability, negligible volatility, and their ability to be chemically tuned through the modification and combination of different ions. In this context, superbase ILs have been studied as CO_2 capture agents in flue gas treatments, as an alternative to the industry standard of alkanolamines, which have known drawbacks, such as a high corrosivity and toxicity.[1] The presence of small amounts of NO_x in these systems degrades the alkanolamine through the formation of nitrosamines, further increasing the corrosivity and toxicity/carcinogenicity, and consequently, decreasing the lifetime of the solvent.[2–4] NO_x and, therefore, NO emissions are regulated (not to exceed 40 $\mu g \cdot m^{-3}$ a year),[5] as they react in the atmosphere to form ozone and acid rain.[6] A primary source of NO_x is from flue gas streams,

which make up 40 % of the NO_x emissions from stationary sources.[6] There is therefore a clear need to study its effect on CO_2 capture sorbents for this application.[7]

Flue gas is estimated to contain by volume, 0.15-0.25 % NO_x and 10-15 % CO_2, with 10 % H_2O, 0.05-0.2 % SO_2, and particulates are also present (dependant on fuel type and operating conditions).[8–10] To capture CO_2 from flue gas, a reactive sorbent with a high affinity is required, and consequently, ILs that chemically absorb CO_2 have been shown to be suitable for this process due to their reversible, and increased capacity, over other conventional, physically absorbing ILs.[11–14] Superbase ILs have recently been shown to absorb CO_2 reversibly, in greater than equimolar amounts, and with minimal viscosity changes.[15] A higher affinity for CO_2, however, means that there is a high probability that the IL will strongly absorb other impurities in waste gas streams, as has been reported in the case of tetraalkylphosphonium ILs with gas feeds containing acidic gases such as SO_2.[16]

To combat the emission of NO_x from waste gas streams, research has focused on the use of traps and selective catalytic reduction (SCR) reactions to reduce emissions and improve air quality. ILs have also been investigated for this purpose. However, only concentrated feeds of NO have been studied for both the physical and chemical absorption of the gas.[17–19] The amount of NO captured by the chemically absorbing superbase IL, trihexyltetradecylphosphonium tetrazolide ($[P_{66614}][Tetz]$), was 4.52 nNO:nIL with a pure feed of NO at 30 °C and 1 atm.[19] The capture of NO at concentrations (<0.25 %) has also been investigated,[20] with the effect of O_2 and H_2O being considered,[21,22] often showing a negative impact on the system, and adversely affecting the reversibility of the system.

For ILs to remain cost-effective for capturing CO_2 in an industrial application, NO must have little effect on the IL, or an effective method of trapping/reducing the NO before exposure of the gas stream to the IL should be used, in order to minimise any negative impacts and extend the sorbents lifetime. In this work, the effect of NO in a combined feed with CO_2 at typical flue gas concentrations was studied. Following on from the promising CO_2 capture results by $[P_{66614}][Benzim]$, in the presence of H_2O and SO_2,[15,16] the superbase IL was further investigated in this work. The interpretation of the experimental findings was assisted by electronic structure, DFT calculations, whereby all possible binding confirmations of the gases

were considered. The calculated energies and spectroscopic data were found to be in excellent agreement with experimental values.

Experimental

Materials

Trihexyltetradecylphosphonium chloride ([P_{66614}]Cl, 97.7 wt.%, CAS: 258864-54-9) was obtained from Iolitech, and benzimidazole (98 wt.%, CAS: 51-17-2) was purchased from Sigma–Aldrich. Gases were obtained from BOC; argon (99.998%, CAS: 7440-37-1); carbon dioxide (99.99%, CAS: 124-38-9); nitric oxide (1 % in argon, CAS: 10102-43-9). [P_{66614}][Benzim] was prepared using a previously reported two-step synthesis method.[15] [P_{66614}][OH] was synthesized using an anion exchange resin from [P_{66614}]Cl followed by addition of the superbase, benzimidazole. The solution was stirred overnight and then dried *in vacuo* (10^{-3} Pa) at 50 °C for at least 96 h. The water content in the studied IL was measured using a Metrohm 787 KF Titrino Karl Fischer machine and was found to be 0.075 wt.%. Halide content was determined to be <5 ppm using a silver nitrate test.[23] The structure and purity of the synthesized IL, and post-absorption, was analysed using ^{1}H-NMR and ^{13}C-NMR with a Bruker Avance II 400 MHz Ultra shield Plus and were carried out as neat ILs in the presence of a glass capillary insert containing deuterated solvent (DMSO-d_6, purchased from Cambridge Isotope Laboratories Inc., CAS: 2206-27-1). Previously published TGA results show this IL has a decomposition temperature of 289 °C (Figure S1).[15]

Methods

Two methods were used to measure the gas uptake in this work (gas concentrations are reported as vol. %). For gravimetric measurements, the IL was weighed out (0.5 g ± 0.1 mg) into a small vial with a septum lid (1.9 cm^3) in an argon-filled glove box. The IL was pre-treated by bubbling with nitrogen at 80 °C at a flow rate of 50 $cm^3 \cdot min^{-1}$ to dry the sample until the weight had stabilized, recorded on an electronic balance with an accuracy of ± 0.1 mg. The sample was then bubbled with either dry 14 % CO_2 in Ar or 1 % NO in Ar, at a flow rate of 40 $cm^3 \cdot min^{-1}$ at 22 ± 0.5 °C. The gas absorption was monitored after 5, 15, 30, 60 mins and then hourly, until the weight stabilised. The weight gain was then used to calculate the amount of

CO_2/NO absorbed (considering the mass of the headspace).[15] The mass of the IL was measured with an uncertainty close to 10^{-4} g leading to an overall uncertainty better than 0.01 nGas:nIL. The desorption was also studied by bubbling the sample with Ar at 80 °C. Each measurement was repeated and values quoted, herein, are an average of at least two experiments.

A second method using a mass spectrometer to monitor the gas phase concentrations was also used. This method has been described in detail previously.[16] 2 g (± 0.1 mg) of IL was weighed out in the glovebox and transferred into a temperature-controlled glass reactor with a gas inlet/outlet. The IL samples were subjected to a number of absorption and desorption cycles. At the start of a cycle, the 2 h absorption period was started by switching the feed stream from Ar to the desired feed composition (typically 14 % CO_2 + 0.2 % NO in Ar at 1 atm (± 0.05 atm)) allowing the IL to be exposed to the gas. Once the absorption period had ended, the desorption period was started by switching the feed stream to Ar and increasing the temperature of the IL to 90 °C for 2 h, until a stable CO_2 (m/z 44) signal was observed. At the end of a cycle, the temperature was cooled to 22 °C (± 0.05 °C). The CO_2 uptake was calculated using the

breakthrough curve obtained from following m/z 44, normalised by m/z 36 (Ar fragment), to account for any drift in the mass spectrometer over time. To validate the technique, a feed of 14 % CO_2 in Ar was used;

three experiments were carried out and the overall uncertainty associated with the measurement was calculated to be ±0.04 nCO_2:nIL.

Analysis

The viscosity of the IL samples was measured before and after NO absorption using a TA Instruments AR2000. Elemental analysis was carried out using a Thermo Scientific Flash 2000 elemental analyser. X-ray Photoelectron Spectroscopy (XPS) was performed with a Kratos AXIS Ultra DLD apparatus, with monochromated Al Kα radiation X-ray source, charge neutralizer and hemispherical electron energy analyser. During data acquisition, the chamber pressure was kept below 10^{-9} mbar. The spectra were analysed using CasaXPS and corrected for charging using the C 1s feature at 284.8 eV.

Attenuated Total Reflectance-Infrared (ATR-IR) spectra were recorded on a ZnSe crystal in a modified *in-situ* cell, using a PIKE ATRMax II accessory and a Bruker Tensor II infrared spectrometer. The ZnSe crystal was coated with a thin film of $[P_{66614}][Benzim]$ (250 mg), before introduction of the gas feed (14 % CO_2 in Ar, 0.2 % NO in Ar, or a mixed gas feed of 14 % CO_2 with 0.2 % NO in Ar (flow rate of 15 $cm^3 \cdot min^{-1}$)). All gases were passed through an acetone-ice bath (-10 °C) before introduction into the cell. The background for all spectra was the ZnSe crystal in the cell and all spectra were recorded with 8 scans at 4 cm^{-1} resolution.

DFT Calculations

Unless otherwise specified, all energies reported here were obtained using a combination of the hybrid functional UB3LYP and the triplet-ζ basis set 6-311++G**.[24,25] This methodology has been used extensively for calculating kinetic and thermodynamic properties of group transfer reactions.[26–28] Additional benchmarking and verification was done using the pure density functional UBP86, and is available in the SI (Tables S11 S16).[24,29] All major trends obtained with the UB3LYP functional were replicated with the pure UBP86 functional. All minimum energy structures were obtained with full optimisation, without constraints. Analytical frequencies were run on each structure at 1 atmosphere pressure and a temperature of 298.15 K and the resulting infrared spectra were compared with experimental data. These calculations also confirm the presence of true local minima structures by the absence of any imaginary frequencies. Corrections for long range non-bonding interactions were given using the Grimme D3 dispersion model,[30] as implemented in the Gaussian09 software package.[31] Absorption energies were calculated as shown in Equation 1, whereby, the sum of the energies of the IL and molecule(s) were subtracted from the adsorbed molecule−IL species.

$$- \quad (\text{IL} \quad) - (\text{IL} + \text{molecule}) \qquad \text{Equation 1}$$

The models consist of one mole of $[Benzim]^-$, as well as the absorbates; whilst the larger models also included a truncated version of the $[P_{66614}]^+$ cation, $[P_{3333}]^+$. An implicit solvent model of acetonitrile was additionally undertaken using a Polarizable Continuum Model (PCM). Acetonitrile with a dielectric

constant of ε = 35.688 was chosen because of its intermediate polarity, which is sufficient to effectively stabilise charged species whilst not unrealistically polarising the SCF. Unless otherwise stated, the energies presented were obtained in the gas phase. However, complete data sets for the solvent corrected values are available in the SI. The starting geometries for the [P_{3333}][Benzim] models were informed by a previous study that utilized NVT dynamics to obtain the lowest energy configurations for the interaction between the cation and anion components of the IL.[32] The molecular visualisation software ChemCraft was then used to add manually the different adsorbate(s) in position to chemically absorb to the IL, before a full optimisation of the resulting species could be undertaken.[33]

Results and Discussion

Initially, the absorption of NO was studied using a gravimetric technique, with [P_{66614}][Benzim] as the sorbent. It was found that with a feed of 1 % NO in argon, 1.73 nNO:nIL was absorbed when left to stabilise for 72 h under the feed (Table S1 in SI). The time required to saturate the IL with NO was significantly longer than for CO_2 (15 mins), which could be due to the lower solubility of NO in the IL.[15] A greater than equimolar absorption of NO was observed, which may be associated with physically/weakly absorbed NO, the absorption of NO on more than one site, or the formation of a NONOate species from two moles of NO absorbing on the same site, as seen for [P_{66614}][Tetz].[19] The desorption of the NO-saturated IL was studied by heating it under argon at 80 °C after which 1.39 nNO:nIL remained, showing that a large proportion of the NO was strongly (chemisorbed) and irreversibly bound to the IL, following the desorption conditions studied. These desorption conditions were the same as applied after CO_2 absorption whereby the ILs absorption capacity was fully restored.[15] The small loss in weight (1.73 to 1.39 nNO:nIL) could be due to removal of physisorbed or weakly bound NO. In contrast, using [P_{66614}][Tetz], 13 h was required for the weight to stabilise with 3.56 nNO:nIL captured (30 °C, 0.1 bar, 100 % NO).[19] 4.52 nNO:nIL was absorbed by [P_{66614}][Tetz] at a higher NO partial pressure (30 °C, 1 atm, 100 % NO), however, 2.79 nNO:nIL remained after desorption (80 °C, 1 atm, N_2), indicating a strongly bound species was also observed.

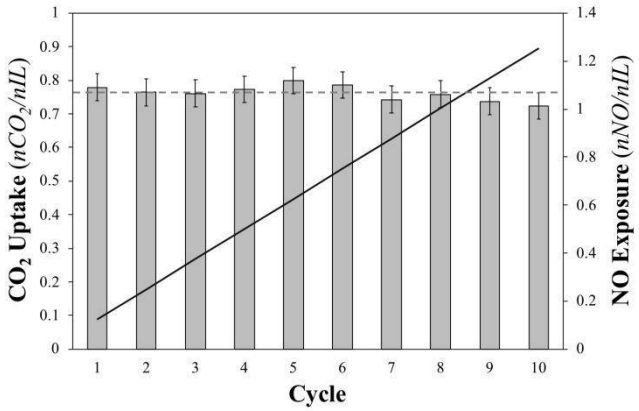

Figure 1. CO_2 capacity (bars) of [P_{66614}][Benzim], calculated from the MS, and calculated exposure to NO (solid line), after multiple cycles of a 2 h absorption under a feed 14 % CO_2 and 0.2 % NO in argon, and a 2 h desorption at 90 °C. Dashed line depicts the 14 % CO_2 only value.

Gravimetric analysis allows for the uptake of a single gas to be studied. However, as waste flue gases are multicomponent, the ability of the IL to absorb CO_2 in the presence of NO needs to be assessed, to do which, the absorption of a co-feed consisting of 14 % CO_2 + 0.2 % NO in Ar by [P_{66614}][Benzim] was studied in a gas absorption rig with an on-line MS (Figure 1 and Table S2 in SI). This system has been previously developed and validated for the uptake of CO_2 + SO_2 feeds.[16] In order for the IL to be exposed to an equivalent number of moles of NO for the amount of IL present (2 g), 10 cycles were carried out; with each cycle consisting of a 2 h absorption period under feed conditions at 22 °C, followed by a 2 h desorption period under argon at 90 °C. The IL was initially pre-treated with a feed containing 14 % CO_2, and an average value of 0.78 nCO_2:nIL was obtained, consistent with the previous work.

[P_{66614}][Benzim] was capable of absorbing large amounts of NO (measured gravimetrically) when exposed to NO as a single component feed. However, the gas absorption rig showed that for a co-feed of CO_2 + NO, CO_2 was able to effectively compete with NO for the absorption sites, with 0.78 nCO_2:nIL still absorbed during the first cycle. Interestingly, after 10 cycles, the CO_2 absorption capacity had only reduced to 0.72 ± 0.04 nCO_2:nIL, and at the equimolar exposure point, [P_{66614}][Benzim] was still able to absorb 0.76 nCO_2:nIL. This compares with 0.17 nCO_2:nIL when the IL was treated with a co-feed containing 14 % CO_2

+ 0.2 % SO_2, showing that [P_{66614}][Benzim] has a significantly higher resistance to poisoning by NO than SO_2 at flue gas concentrations.[16]

Characterisation of [P_{66614}][Benzim] post-absorption was required to examine the mode of absorption of NO and its effect on the physical properties of the IL. All post-absorption characterisation was performed on the IL after 10 absorption/desorption cycles of the 14 % CO_2 + 0.2 % NO feed, with the final desorption step performed to remove any absorbed CO_2 and physisorbed NO. The effect of the absorption cycles on the viscosity of [P_{66614}][Benzim] was investigated (Table S3 in SI). It was previously reported that the absorption of CO_2 resulted in a decrease in viscosity from 1149 to 388 mPa·s.[15] However, after 10 absorption/desorption cycles of the 14 % CO_2 + 0.2 % NO co-feed, an increase in the viscosity was observed, from 1087 to 1235 mPa·s. This increase was associated with the absorption of NO and was likely due to an increase in hydrogen bonding between the [Benzim-NO]$^-$ species and the phosphonium cation. The absorption of the CO_2 + NO co-feed showed NO to have little effect on the CO_2 absorption capacity of the superbase IL and correspondingly, elemental analysis of the IL post 10 cycles (Table S3 in SI) showed only a small increase in nitrogen content, from 6.10 to 6.48 wt.%, likely due to a chemisorbed species being retained in the IL after desorption.

^{1}H and ^{13}C NMR spectra of [P_{66614}][Benzim] (Figure S2 and S3 in SI, respectively) before and after exposure to 1 % NO, and the 14 % CO_2 + 0.2 % NO co-feed, showed a downfield shift in the protons (and carbon atoms) in the anion ring when comparing the IL before and after exposure to NO, which was indicative of the chemical absorption of NO to the anion and was observed previously with CO_2 and SO_2.[15,16] This shift was not observed in the co-feed treated sample due to the small amount of NO absorbed. The chemisorbed species gave a new contribution in the N 1s region at 402.4 eV in the XPS spectrum of the IL, post-absorption (Figure S4 in SI), which was likely due to the absorption of a small amount of NO to yield either an NO or N_2O_2 species, reported to have photoelectron peaks at 401.2 and 403.0 eV respectively, in the literature.[34,35] All the co-feed post-absorption characterisation corroborate the experimental results where NO was found to have little effect on the CO_2 capacity; however, a change in the amount of irreversibly bound species was observed gravimetrically. Therefore, *in-situ* ATR-IR

spectroscopy was used to identify the species formed during the absorption of NO alone and for CO_2 in the presence of NO. The data are presented predominantly as difference spectra where the $[P_{66614}]$[Benzim] IL before introduction of the feed gases (NO, or the co-feed), has been subtracted from the spectra recorded under the feed gases at different exposure times to highlight the changes due to the absorption of the gases.

The gravimetric study showed a greater than equimolar absorption of NO, which was irreversibly absorbed with only 0.34 nNO:nIL removed, after desorption at 90 °C under Ar. Therefore, an initial study of the absorption of 0.2 % NO in Ar was performed to probe the mode of binding of NO to the IL (Figure 2i (a)). New bands in the 1450-1200 cm^{-1} region formed upon the absorption of NO by the IL and it was clear that a number of bands, notably at 1336 and 1309 cm^{-1}, increased at different rates, suggesting that more than one species was forming. The 1336 cm^{-1} band increased initially during the first 0-8 mins of exposure, after which the 1309 cm^{-1} band began to increase, reaching a similar intensity to the 1336 cm^{-1} band after 15 mins of exposure.

During the first 0-8 mins of exposure to NO (Figure 2i (b)), bands were observed to increase at 1374, 1336, 1231, and 933 cm^{-1}. The vibrations at 1374 and 1336 cm^{-1} were assigned to an asymmetric and symmetric (O-N-N-O) stretch of a diazeniumdiolate (NONOate) species (Figure 2ii), with the (N-N) stretch of this species also observed at 933 cm^{-1}.[19,36] The band growing at 1231 cm^{-1} was assigned to the (R_2N^1-N) stretch of a NONOate species chemically absorbed to the N^1 nitrogen site on the benzimidazolide anion,[36] the same absorption site as for the carbamate species formed from CO_2 absorption (Figure S5 in SI). The vibrations at 1374 and 1336 cm^{-1} could also be assigned to the (N-O) stretch of a nitrosamine species, however, it has been shown that NO interacts very weakly with the IL and NONOate formation was more likely.[37–39]

After ~8 mins of exposure, the 1309 cm^{-1} band increased more rapidly as the growth in the 1336 cm^{-1} band slowed, indicative of the growth of a second species. Subtracting the 8 min exposure spectrum from all further spectra (Figure 2i (c)), highlighted that the bands correlated with the 1309 cm^{-1} species with a band found at 1400 cm^{-1}, which together were assigned to the asymmetric and symmetric stretch of a NONOate species, absorbed onto a second site of the benzimidazole anion, denoted the N^2 position (Figure

2ii). It was proposed that NO could have multiple modes of binding with superbase ILs,[19] which is in agreement with the greater than equimolar absorption of NO found gravimetrically in this study. Further bands associated with the NONOate species at the N^2 position were observed in the 870 - 827 cm^{-1} region, due to a shift in the NONOate (N-N) vibration upon absorption onto the second site.[19,36] The faster formation of the first NONOate species, eventually followed by a second, would suggest strong absorption for the first site and a weaker absorption on the second site.

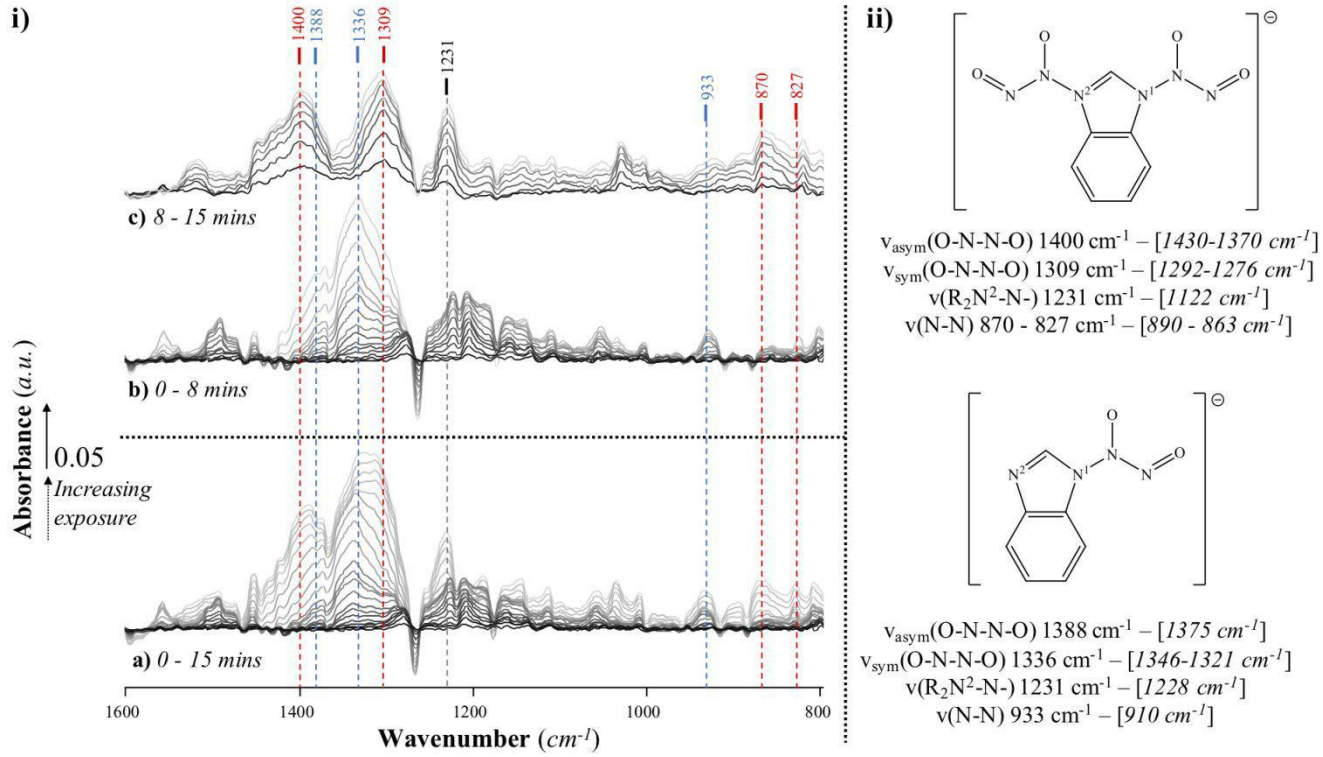

Figure 2. i) ATR-IR subtracted spectra of $[P_{66614}][Benzim]$ showing 15 mins of exposure to a feed of (a) 0.2 % NO in Ar. Further subtractions were carried out for (b) 0-8 mins and (c) 8-15 mins. *n.b. The scan after 8 mins in (b) was further subtracted from succeeding spectra to show the formation of a NONOate species binding to the second site of the anion.* Carried out at 22 °C with a flow rate of 15 $cm^3 \cdot min^{-1}$. – N^1-N(O)NO – N^2-N(O)NO. Fully labelled spectra can be found in Figure S5 in SI. **ii)** Depicts the experimentally observed, and [theoretically derived] IR vibrations, when $[P_{66614}][Benzim]$ absorbs NO to form NONOate species bound to different sites on the anion.

In order to confirm the proposed mode of NO absorption, DFT calculations were performed to calculate the binding energy of NO to a truncated [P_{3333}][Benzim] model. The results, displayed in Table 1, show that the NONOate species had a higher affinity for binding to the IL, than a single molecule of NO, by approximately 61 kJ·mol^{-1}. It also shows that a second NONOate species is able to bind to the N^2 position on the anion. However, the difference in energies (-49.46 *vs.* -91.09 kJ·mol^{-1}) indicates that a weaker bond is formed upon absorption at the N^2 site. The computational model strongly supported the infrared characterisation, with the calculated bands shown in square brackets in Figure 2ii. Furthermore, it was impossible to assign computationally the observed vibrations to the absorption of a single molecule of NO by the IL.

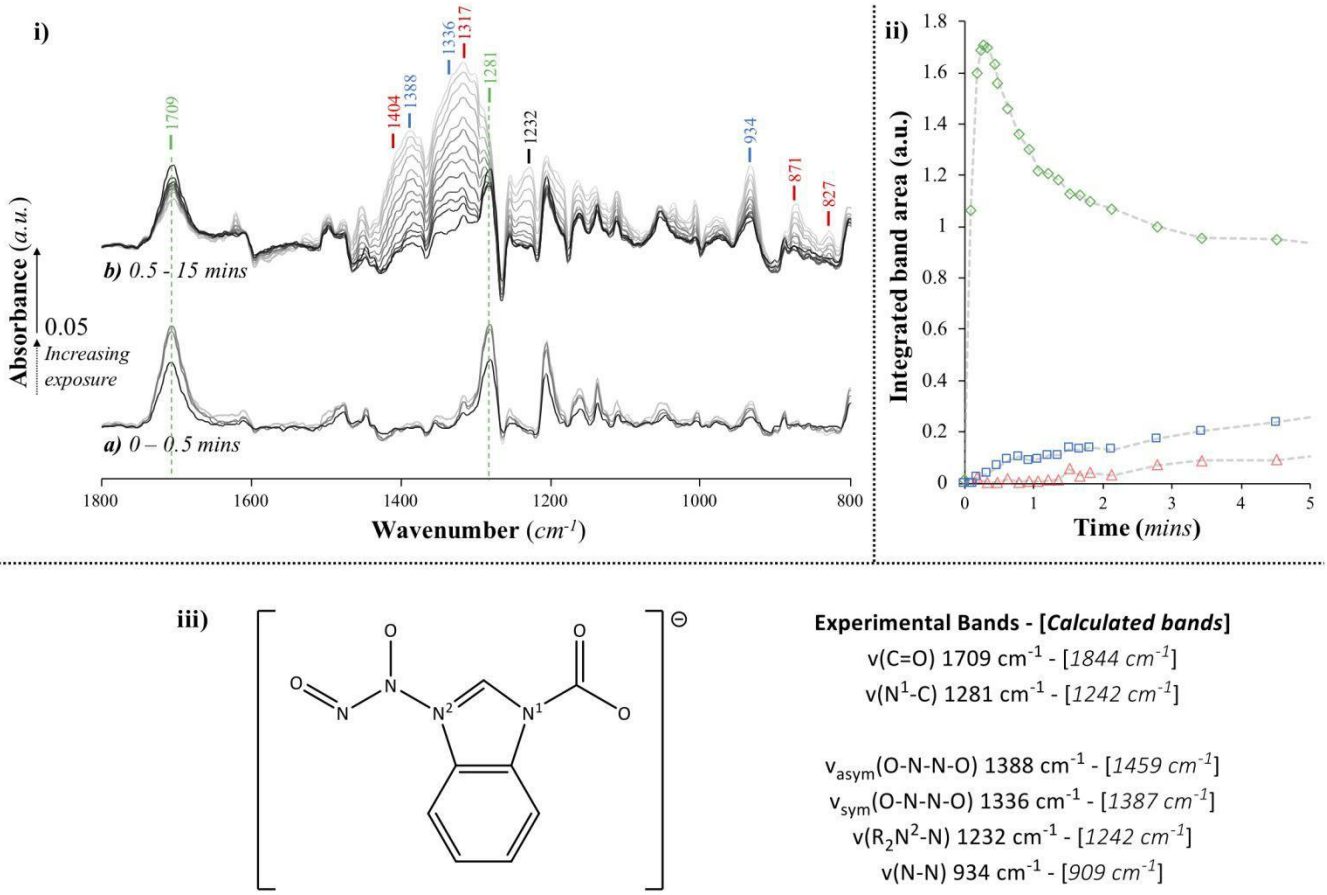

Figure 3. i) ATR-IR subtracted spectra of [P_{66614}][Benzim] showing exposure to a co-feed of 14 % CO_2 + 0.2 % NO in Ar for a) 0 - 0.5 mins b) 0.5 – 15 mins. Carried out at 22 °C with a flow rate of 15 cm^3·min^{-1}. – N^1-N(O)NO – N^2-N(O)NO – CO_2. **ii)** Integrated band areas for ◇ N^1-CO_2 (1709 cm^{-1}) , □ N^1-NONO

(933 cm^{-1}) and △ N^2-NONO (870-827 cm^{-1}), under a co-feed of 14 % CO_2 + 0.2 % NO in Ar for 0-5 mins at 22 °C. **iii)** Depicts the experimentally observed, and theoretically derived IR vibrations, when [P_{66614}][Benzim] absorbs CO_2 and NO after exposure to a co-feed of 14 % CO_2 + 0.2 % NO in Ar.

NO was then studied in a co-feed with CO_2. Figure 3i (a) initially indicates a rapid increase in the bands at 1709 cm^{-1} (C=O), and 1281 cm^{-1} ($N\text{-}COO^-$) for the carbamate species,[14,16,40,41] even in the presence of 0.2 % NO, which is probably due to the higher concentration of CO_2 (14 %) in the feed compared with NO. This high level of CO_2 absorption however, was not maintained over the time of exposure, with the carbamate bands then decreasing as bands due to the NONOate species binding at the N^1 site increased. (Figure 3i (b)). The initial drop in the CO_2 bands suggest the displacement of absorbed CO_2 by NO. However, NO does not fully displace all the absorbed CO_2 as a reduced, but stable, integrated band area for the carbamate C=O stretch (1709 cm^{-1}) is observed from ~3-90 mins of exposure to the co-feed (Figure 3ii and Figure S6 in SI). A NONOate absorbed at the N^2 position also increases with exposure time, suggesting that NO can bind to the N^2 site with either a CO_2 or NONOate species absorbed at the N^1 site (Figure 3iii). The stabilisation of the integrated band intensities for the NONOate species (N^1 and N^2) as well as the carbamate species (Figure 3ii), show that [P_{66614}][Benzim] can maintain capacity for CO_2 absorption after exposure to a co-feed where NO is in low concentration, consistent with the gas absorption rig data.

From the calculated energies of absorption for NONO and CO_2, of -91.09 and -52.12 $kJ{\cdot}mol^{-1}$, respectively (Table 1), it would be expected that a NONOate species would be absorbed more strongly than CO_2, which is reflected in the gravimetric results where NO binds irreversibly, while CO_2 undergoes reversible absorption. Importantly, this trend is replicated with the anion only, implicit solvent model and also the UBP86 models (see SI Tables S4 S16). However, in a co-feed where CO_2 is in a significantly higher concentration than NO (realistic concentrations for a waste gas stream applications) the two gases can compete well for absorption sites which reduces the expected poisoning effect of NO. The changes in the CO_2 bands in the presence of NO indicate that as the concentration of NO in the IL increases, at a limiting concentration it can out-compete CO_2 for binding at the N^1 site, due to the stronger binding of a NONOate compared to CO_2. This stronger absorption is corroborated by the stability of the NONOate bands

to desorption, under Ar at 90 °C (Figure S7 in SI), where the carbamate bands are removed with little change in the intensity of the NONOate bands.

Furthermore, since the theoretical model also shows a preference for the co-binding of CO_2 and NONO, over that of two moles of the NONOate, it would be expected that thermodynamic factors would favour much slower deactivation of the IL by NO. In comparison, SO_2 has a significantly higher exothermic absorption energy compared to CO_2 (and NO) which resulted in the rapid removal of carbamate bands in under 5 mins of exposure to a co-feed of CO_2 and SO_2 in equivalent ATR experiments.[16] Using the computationally derived absorption energies, the binding of the NONOate was assessed as being intermediate between the reversible adsorption of CO_2 and the irreversible absorption of SO_2. The strongly exothermic nature of the chemisorption of CO_2, NO, and SO_2, is shown in Figure S8 (in SI). The electrostatic potentials of the IL, coupled to each absorbate, has been analysed and shows the strongly chemisorbed nature of each species (Figure S9 in SI).[42] The addition of the $[P_{3333}]^+$ truncated cation and the inclusion of the PCM solvent correction systematically lowered all absorption energies. However, the general trend remains the same in all models and are replicated with both functionals (see S4 S16 in SI), which is to be expected because the stabilization of the anion by either the cation or a polar solvent will inevitably decrease the amount of stabilization obtained by the absorbate binding. Additionally, the absorption energies correlate very well with the amount of charge transfer from the IL to the adsorbate, with ordering of CO_2 > NONO > SO_2. Therefore, in general the lower the amount of charge transfer, the stronger the chemical adsorption.

Table 1. Gas phase absorption energies for various absorbates to a model of [P_{3333}][Benzim] IL. All energies were obtained at B3LYP/6-311++G** level of theory and are given in kJ·mol^{-1}. Enthalpies (**E**) and free energies (**G**) are both given, with the subscript, ZPE, representing the zero-point corrected values.

	E	**E_{ZPE}**	**ΔG**
[Benzim]CO_2	-63.81	-52.12	-9.60
[Benzim]NO	-32.44	-29.61	+5.47
[Benzim]NONO	-105.95	-91.09	-33.15
[Benzim]2NONO	-76.48	-49.46	+64.46
[Benzim](CO_2)NONO	-82.43	-60.35	+41.59
[Benzim]SO_2	-134.22	-123.89	-69.50

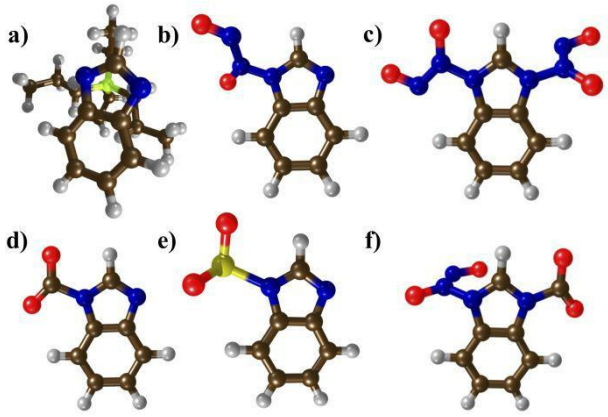

Figure 4. Depicts a model of the [Benzim]$^-$ anion in a) [P_{3333}][Benzim], absorbing b) one mole of NONO, c) two moles of NONO, d) one mole of CO_2, e) one mole of SO_2, and f) one mole of CO_2 and NONO.

Conclusions

The effect of NO on the CO_2 uptake capacity of [P_{66614}][Benzim] was characterised in this work, using absorption measurement techniques, a range of physical property measurements, and *in-situ* infrared spectroscopy. The absorption of NO was shown to form NONOate species with multi-site bonding to the [Benzim]$^-$ anion shown in the infrared, also corroborated by DFT calculations. With a co-feed of 14 % CO_2 + 0.2 % NO, NO was found to have a little effect on the CO_2 capacity of the IL, with [P_{66614}][Benzim] still reversibly absorbing 0.72 ± 0.04 nCO_2:nIL after 10 absorption/desorption cycles, showing good competition between the gases, however, NO was still found to bind irreversibly to the IL in small amounts over time. Increases in the nitrogen content and viscosity of the IL further showed the chemisorption of NO, confirmed using spectroscopic techniques (^{1}H NMR, ^{13}C NMR, and XPS).

DFT calculations found that, for the modelled IL, the binding energy strength was in the order of SO_2 >> N(O)NO > CO_2 > NO. This correlated well with the observed results, where SO_2 was previously found to displace CO_2 from the IL, with NO absorption as a NONOate species occurring more slowly. At the concentrations used in this study, CO_2 could compete with NO at the studied exposure times and complete displacement of the carbamate was not observed, in contrast to CO_2 + SO_2. These results indicate that an alternative upstream/downstream process, such as a regenerable NO_x trap or SCR reaction, could be utilized in order to lower the concentration of NO in the feed, and lengthen the lifetime of the IL for the efficient absorption of CO_2. It is recognised that the effects of NO_2 or O_2/H_2O in the feed should also be considered and will be addressed in future work, however, this study has shown that [P_{66614}][Benzim] can efficiently capture CO_2 from waste gas streams, in the presence of NO, at realistic waste flue gas stream concentrations.

SUPPORTING INFORMATION

The supporting information is available free of charge on the ACS Publications website at: http://pubs.acs.org.

Experimental data of gravimetric results (Table S1); the CO_2 uptake values, by [P_{66614}][Benzim], in the presence of NO (Table S2) and subsequent property analysis (Table S3); NMR data, and ^{1}H/^{13}C NMR

spectra (Figure S1 and S2, respectively); XPS data (Figure S3); ATR-IR difference spectra of the absorption of CO_2 and NO individually (Figure S4) and integrated band areas for the absorption of the CO_2 + NO co-feed over 90 min (Figure S5); ATR-IR spectra showing desorption of the NO only feed, and the NO + CO_2 co-feed (Figure S6); the absorption energies for various gases to models of the $[P_{66614}]$[Benzim] IL (Tables S4 to S16); Calculated IR frequencies compared with experimental observations (Table S17); listed cartesian coordinates.

ACKNOWLEDGEMENTS

The authors acknowledge funding from the EPSRC under the grant no. EP/N009533/1, a multi-disciplinary approach to generating low carbon fuels, carried out in collaboration with the University of Manchester, Queen's University Belfast, Cardiff University and University College London. Open access data can be found via the University of Manchester research portal. AJG further acknowledges funding from the Department of Employment and Learning. Computing facilities for this work were provided by ARCCA at Cardiff University, HPC Wales, and through membership of the UK's Materials Chemistry Consortium (MCC). The MCC is funded by the EPSRC (EP/F067496).

NOTES

The authors declare no competing financial interest.

REFERENCES

1. Brennecke, J. F. & Gurkan, B. E. Ionic Liquids for CO_2 Capture and Emission Reduction. *J. Phys. Chem. Lett.* **2010**, *1*, 3459–3464, DOI 10.1021/jz1014828.

2. Fostås, B., Gangstad, A., Nenseter, B., Pedersen, S., Sjøvoll, M. & Sørensen, A. L. Effects of NO_x in the flue gas degradation of MEA. *Energy Procedia* **2011**, *4*, 1566–1573, DOI 10.1016/J.EGYPRO.2011.02.026.

3. Supap, T., Shi, H., Idem, R., Gelowitz, D., Campbell, C. & Ball, M. Nitrosamine Formation Mechanism in Amine-Based CO_2 Capture: Experimental Validation. *Energy Procedia* **2017**, *114*, 952–958, DOI 10.1016/J.EGYPRO.2017.03.1239.

4. Magee, P. N. & Barnes, J. M. The production of malignant primary hepatic tumours in the rat by feeding dimethylnitrosamine. *Br. J. Cancer* **1956**, *10*, 114–122, DOI 10.1038/bjc.1956.15.

5. European Parliament Directive 2008/50/EC of 21 May 2008 on ambient air quality and cleaner air for Europe [Online]. [Accessed 22 October 2018]. Available at: https://eur-lex.europa.eu/.

6. Clean Air Technology Centre. Nitrogen Oxides (NO_x), Why and How They Are Controlled. **1999**, *800*, 553–6847.

7. Delmas, R., Serça, D. & Jambert, C. Global inventory of NO_x sources. *Nutr. Cycl. Agroecosystems* **1997**, *48*, 51–60, DOI 10.1023/A:1009793806086.

8. Khatri, R., Chuang, S., Soong, Y. & Gray, M. Thermal and Chemical Stability of Regenerable Solid Amine Sorbent for CO_2 Capture. *Energy & Fuels* **2006**, *20*, 1514–1520, DOI 10.1021/ef050402y.

9. Ertl, G. & Knoezinger, H. *Handbook of Heterogeneous Catalysis, vol. 5*. (Wiley-VCH, 1997), DOI 10.1002/9783527619474.

10. Gao, J., Wang, S., Zhao, B., Qi, G. & Chen, C. Pilot-scale experimental study on the CO_2 capture process with existing of SO_2: Degradation, reaction rate, and mass transfer. *Energy and Fuels* **2011**,

*25***,** 5802–5809, DOI 10.1021/ef2010496.

11. Zhang, Y., Zhang, S., Lu, X., Zhou, Q., Fan, W. & Zhang, X. Dual amino-functionalised phosphonium ionic liquids for CO_2 capture. *Chemistry* **2009**, *15***,** 3003–3011, DOI 10.1002/chem.200801184.

12. Gurkan, B. E., de la Fuente, J. C., Mindrup, E. M., Ficke, L. E., Goodrich, B. F., Price, E. A., Schneider, W. F. & Brennecke, J. F. Equimolar CO_2 Absorption by Anion-Functionalized Ionic Liquids. *J. Am. Chem. Soc.* **2010**, *132***,** 2116–2117, DOI 10.1021/ja909305t.

13. Blath, J., Deubler, N., Hirth, T. & Schiestel, T. Chemisorption of carbon dioxide in imidazolium based ionic liquids with carboxylic anions. *Chem. Eng. J.* **2012**, *181–182***,** 152–158, DOI 10.1016/j.cej.2011.11.042.

14. Wang, C., Luo, X., Luo, H., Jiang, D. E., Li, H. & Dai, S. Tuning the basicity of ionic liquids for equimolar CO_2 capture. *Angew. Chemie - Int. Ed.* **2011**, *50***,** 4918–4922, DOI 10.1002/anie.201008151.

15. Taylor, R., McCrellis, C., McStay, C., Jacquemin, J., Hardacre, C., Mercy, M., Bell, R. G. & de Leeuw, N. H. CO_2 Capture in Wet and Dry Superbase Ionic Liquids. *J. Solution Chem.* **2015**, *44***,** 511–527, DOI 10.1007/s10953-015-0319-z.

16. Taylor, S. F. R., McClung, M., McReynolds, C., Daly, H., Greer, A. J., Jacquemin, J. & Hardacre, C. Understanding the Competitive Gas Absorption of CO_2 and SO_2 in Superbase Ionic Liquids. *Ind. Eng. Chem. Res.* **2018**, *57***,** 17033–17042, DOI 10.1021/acs.iecr.8b03623.

17. Duan, E., Guo, B., Zhang, D., Shi, L., Sun, H. & Wang, Y. Absorption of NO and NO_2 in Caprolactam Tetrabutyl Ammonium Halide Ionic Liquids. *J. Air Waste Manage. Assoc.* **2011**, *61***,** 1393–1397, DOI 10.1080/10473289.2011.623635.

18. Jiang, B., Lin, W., Zhang, L., Sun, Y., Yang, H., Hao, L. & Tantai, X. 1,3-Dimethylurea

Tetrabutylphosphonium Bromide Ionic Liquids for NO Efficient and Reversible Capture. *Energy & Fuels* **2016**, *30***,** 735–739, DOI 10.1021/acs.energyfuels.5b01826.

19. Chen, K., Shi, G., Zhou, X., Li, H. & Wang, C. Highly Efficient Nitric Oxide Capture by Azole-Based Ionic Liquids through Multiple-Site Absorption. *Angew. Chemie Int. Ed.* **2016**, *55***,** 14364–14368, DOI 10.1002/anie.201607528.

20. Sun, Y., Ren, S., Hou, Y., Zhang, K. & Wu, W. Absorption of nitric oxide in simulated flue gas by a metallic functional ionic liquid. *Fuel Process. Technol.* **2018**, *178***,** 7–12, DOI 10.1016/J.FUPROC.2018.05.012.

21. Kunov-Kruse, A. J., Thomassen, P. L., Riisager, A., Mossin, S. & Fehrmann, R. Absorption and Oxidation of Nitrogen Oxide in Ionic Liquids. *Chem. - A Eur. J.* **2016**, *22***,** 11745–11755, DOI 10.1002/chem.201601166.

22. Li, X., Zhang, L., Li, L., Hu, Y., Liu, J., Xu, Y., Luo, C. & Zheng, C. NO Removal from Flue Gas Using Conventional Imidazolium-Based Ionic Liquids at High Pressures. *Energy & Fuels* **2018**, *32***,** 6039–6048, DOI 10.1021/acs.energyfuels.8b00154.

23. Oster, K., Goodrich, P., Jacquemin, J., Hardacre, C., Ribeiro, A. P. C. & Elsinawi, A. A new insight into pure and water-saturated quaternary phosphonium-based carboxylate ionic liquids: Density, heat capacity, ionic conductivity, thermogravimetric analysis, thermal conductivity and viscosity. *J. Chem. Thermodyn.* **2018**, *121***,** 97–111, DOI 10.1016/J.JCT.2018.02.013.

24. Becke, A. D. Density-functional thermochemistry. III. The role of exact exchange. *J. Chem. Phys.* **1993**, *98***,** 5648–5652, DOI 10.1063/1.464913.

25. Lee, C., Yang, W. & Parr, R. G. Development of the Colle-Salvetti correlation-energy formula into a functional of the electron density. *Phys. Rev. B* **1988**, *37***,** 785–789, DOI 10.1103/PhysRevB.37.785.

26. Sahu, S., Quesne, M. G., Davies, C. G., Dürr, M., Ivanović-Burmazović, I., Siegler, M. A., Jameson, G. N. L., De Visser, S. P. & Goldberg, D. P. Direct observation of a nonheme iron(IV)-oxo complex that mediates aromatic C-F hydroxylation. *J. Am. Chem. Soc.* **2014**, *136***,** 13542–13545, DOI 10.1021/ja507346t.

27. Neu, H. M., Yang, T., Baglia, R. A., Yosca, T. H., Green, M. T., Quesne, M. G., de Visser, S. P. & Goldberg, D. P. Oxygen-Atom Transfer Reactivity of Axially Ligated Mn(V)–Oxo Complexes: Evidence for Enhanced Electrophilic and Nucleophilic Pathways. *J. Am. Chem. Soc.* **2014**, *136***,** 13845–13852, DOI 10.1021/ja507177h.

28. Timmins, A., Quesne, M. G., Borowski, T. & de Visser, S. P. Group Transfer to an Aliphatic Bond: A Biomimetic Study Inspired by Nonheme Iron Halogenases. *ACS Catal.* **2018**, *8***,** 8685–8698, DOI 10.1021/acscatal.8b01673.

29. Perdew, J. P. Density-functional approximation for the correlation energy of the inhomogeneous electron gas. *Phys. Rev. B* **1986**, *33***,** 8822–8824, DOI 10.1103/PhysRevB.33.8822.

30. Grimme, S., Antony, J., Ehrlich, S. & Krieg, H. A consistent and accurate *ab initio* parametrization of density functional dispersion correction (DFT-D) for the 94 elements H-Pu. *J. Chem. Phys.* **2010**, *132***,** 154104, DOI 10.1063/1.3382344.

31. Frisch, M. J., Trucks, G. W., Schlegel, H. B., Scuseria, G. E., Robb, M. A., Cheeseman, J. R., G. Scalmani, V. B., Mennucci, B., Petersson, G. A., Nakatsuji, H., Caricato, M., Li, X., Hratchian, H. P., Izmaylov, A. F., Bloino, J., Zheng, G., Sonnenberg, J. L., Hada, M., Ehara, M., Toyota, K., Fukuda, R., Hasegawa, J., Ishida, M., Nakajima, T., Honda, Y., Kitao, O., Nakai, H., Vreven, T., Montgomery, J. A., Peralta, J. E., Ogliaro, F., Bearpark, M., Heyd, J. J., Brothers, E., Kudin, K. N., Staroverov, V. N., Kobayashi, R., Normand, J., Raghavachari, K., Rendell, A., Burant, J. C., Iyengar, S. S., Tomasi, J., Cossi, M., Rega, N., Millam, J. M., Klene, M., Knox, J. E., Cross, J. B., Bakken, V., Adamo, C., Jaramillo, J., Gomperts, R., Stratmann, R. E., Yazyev, O., Austin, A. J.,

Cammi, R., Pomelli, C., Ochterski, J. W., Martin, R. L., Morokuma, K., Zakrzewski, V. G., Voth, G. A., Salvador, P., Dannenberg, J. J., Dapprich, S., Daniels, A. D., Farkas, Foresman, J. B., Ortiz, J. V, Cioslowski, J. & Fox, D. J. Gaussian 09, Revis. B.01, Gaussian, Inc., Wallingford CT, 200.

32. Mercy, M., Rebecca Taylor, S. F., Jacquemin, J., Hardacre, C., Bell, R. G. & De Leeuw, N. H. The addition of CO_2 to four superbase ionic liquids: a DFT study. *Phys. Chem. Chem. Phys.* **2015**, *17*, 28674–28682, DOI 10.1039/c5cp05153c.

33. Zhurko, G. & Zhurko, D. Chemcraft Program. Academic Version 1.5. **2004**.

34. Sysoev, V. I., Okotrub, A. V., Gusel'nikov, A. V., Smirnov, D. A. & Bulusheva, L. G. In situ XPS Observation of Selective NO_x Adsorption on the Oxygenated Graphene Films. *Phys. status solidi* **2018**, *255*, 1700267, DOI 10.1002/pssb.201700267.

35. Ruiz-Soria, G., Pérez Paz, A., Sauer, M., Mowbray, D. J., Lacovig, P., Dalmiglio, M., Lizzit, S., Yanagi, K., Rubio, A., Goldoni, A., Ayala, P. & Pichler, T. Revealing the Adsorption Mechanisms of Nitroxides on Ultrapure, Metallicity-Sorted Carbon Nanotubes. *ACS Nano* **2014**, *8*, 1375–1383, DOI 10.1021/nn405114z.

36. Keefer, L. K., Flippen-Anderson, J. L., George, C., Shanklin, A. P., Dunams, T. M., Christodoulou, D., Saavedra, J. E., Sagan, E. S. & Bohle, D. S. Chemistry of the Diazeniumdiolates I. Structural and Spectral Characteristics of the [N(O)NO]− Functional Group. *Nitric Oxide* **2001**, *5*, 377–394, DOI 10.1006/NIOX.2001.0359.

37. Piskorz, M. & Urbanski, T. *Ultraviolet and Infrared Spectra of Some Nitrosamines*. *Bulletin de L'Academie, Polonaise Des Sciences, Serie des sciences chimiques* (1963). *XI*.

38. Colthup, N. B., Daly, L. H. & Wiberley, S. E. *Introduction to Infrared and Raman spectroscopy*. (Academic Press, 1990).

39. Haszeldine, R. N. & Jander, J. Further Remarks on the Spectra of Nitrites and Nitrosamines. *J.*

Chem. Phys. **1955**, *23***,** 979, DOI 10.1063/1.1742168.

40. Kamrath, M. Z., Relph, R. A. & Johnson, M. A. Vibrational predissociation spectrum of the carbamate radical anion, $C_5H_5N\text{-}CO_2^-$, generated by reaction of pyridine with $(CO_2)_m^-$. *J. Am. Chem. Soc*. **2010**, *132***,** 15508–15511, DOI 10.1021/ja1073036.

41. Gurkan, B., Goodrich, B. F., Mindrup, E. M., Ficke, L. E., Massel, M., Seo, S., Senftle, T. P., Wu, H., Glaser, M. F., Shah, J. K., Maginn, E. J., Brennecke, J. F. & Schneider, W. F. Molecular Design of High Capacity, Low Viscosity, Chemically Tunable Ionic Liquids for CO_2 Capture. *J. Phys. Chem. Lett.* **2010**, *1***,** 3494–3499, DOI 10.1021/jz101533k.

22
23

42. Lu, T. & Chen, F. Multiwfn: A multifunctional wavefunction analyzer. *J. Comput. Chem.* **2012**, *33***,** 580–592, DOI 10.1002/jcc.22885.

TOC – For Table of Contents Only

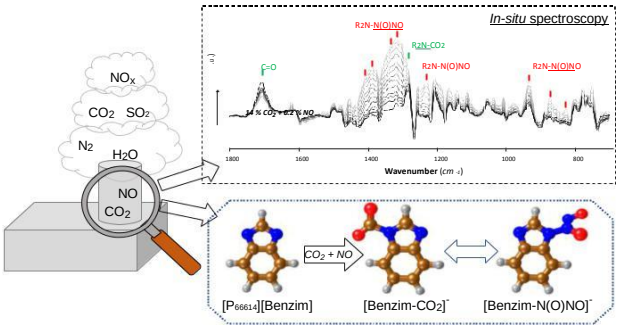

Synopsis

Superbase ionic liquids are shown to efficiently capture CO_2 in the presence of NO under realistic waste gas stream concentrations.

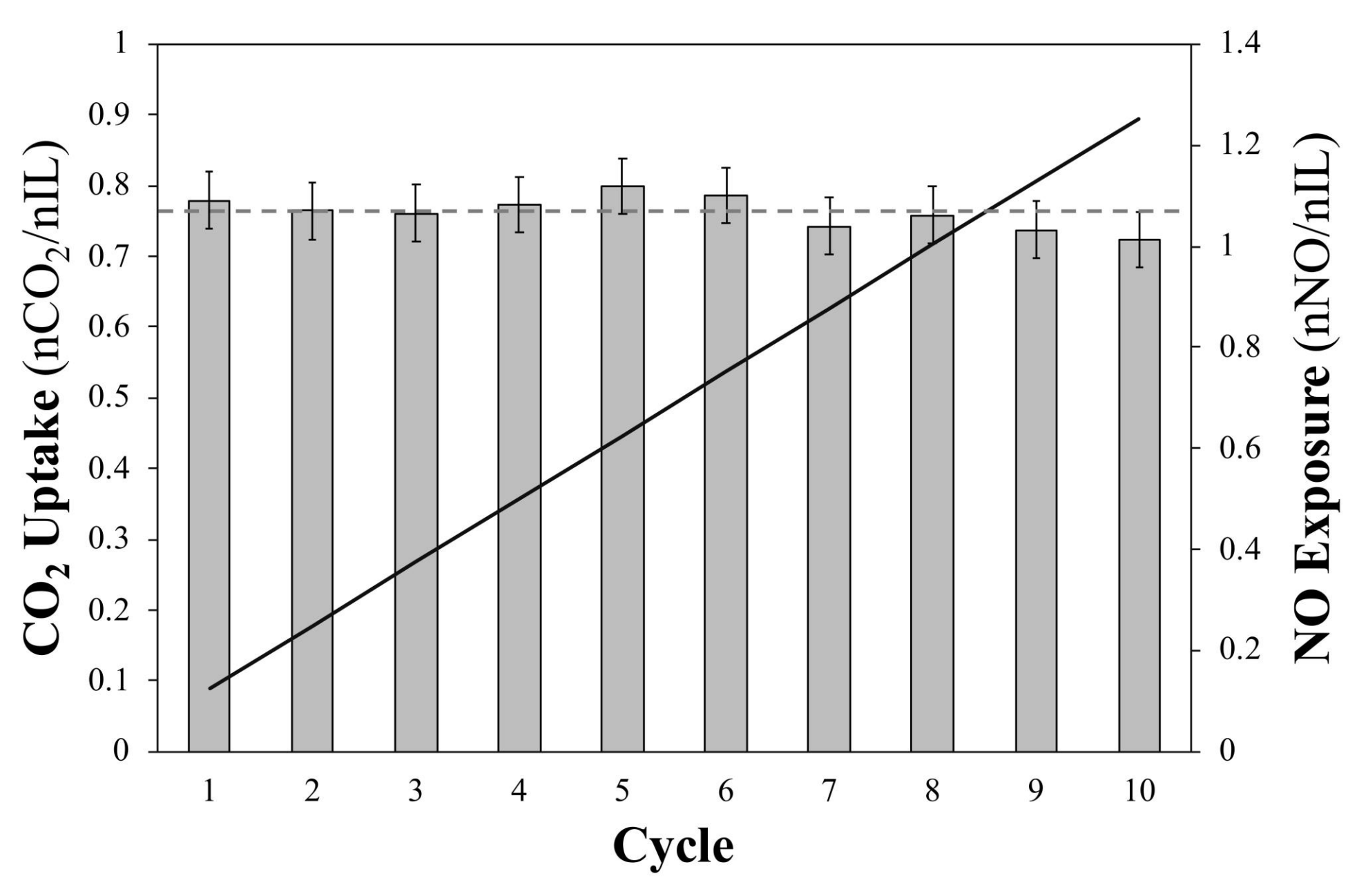
1
0.9
0.8
0.7
0.6
0.5
0.4
0.3
0.2
0.1
0
CO_2 Uptake (nCO_2/nIL)
1.4
1.2
1
0.8
0.6
0.4
0.2
0
NO Exposure (nNO/nIL)
1
2
3
4
5
6
7
8
9
10
Cycle

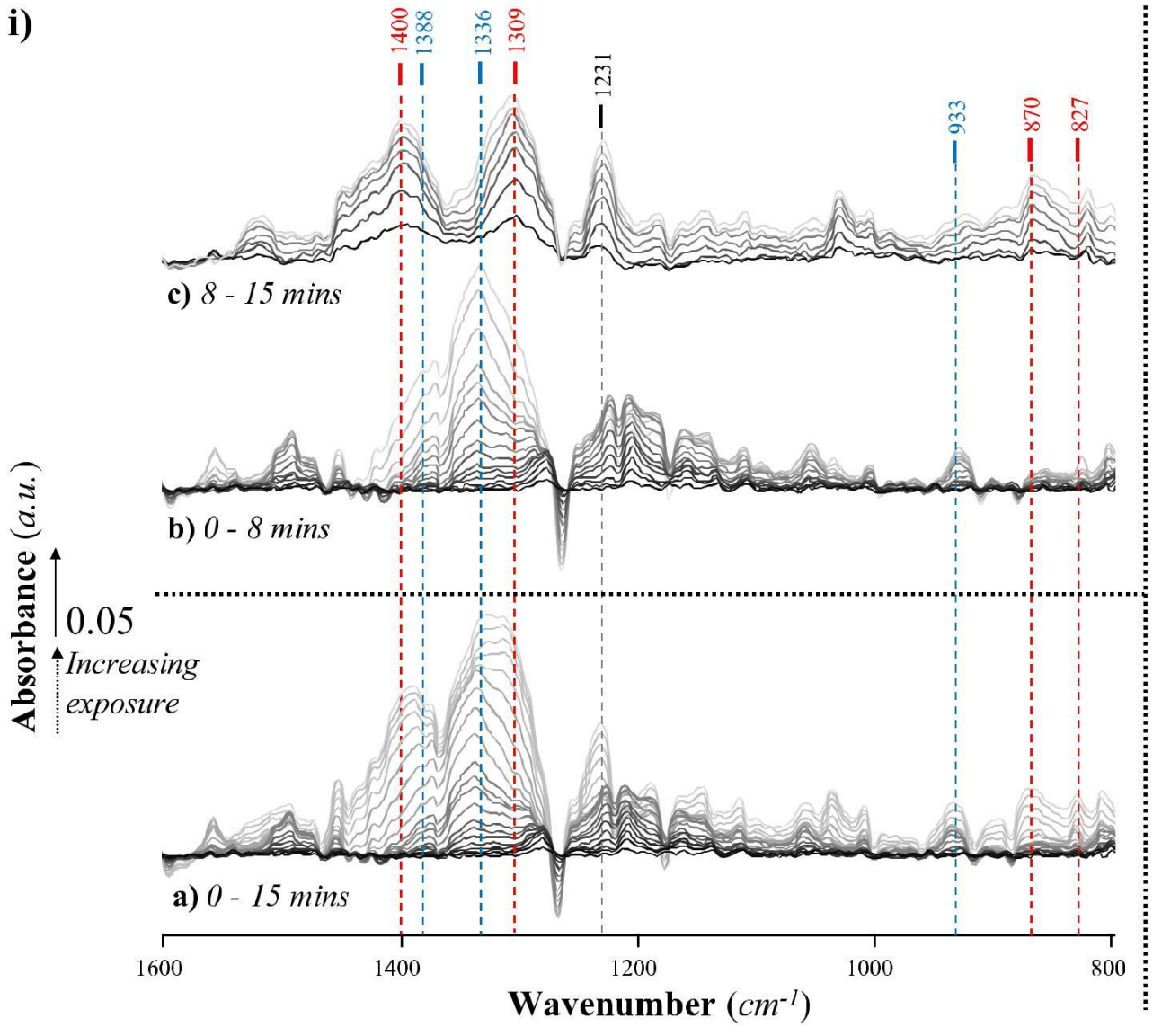

ii)

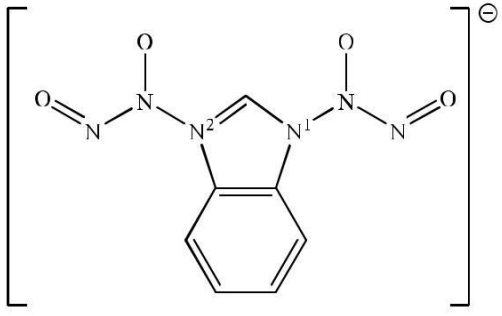

ν_{asym}(O-N-N-O) 1400 cm^{-1} – [*1430-1370 cm^{-1}*]
ν_{sym}(O-N-N-O) 1309 cm^{-1} – [*1292-1276 cm^{-1}*]
$\nu(R_2N^2\text{-}N\text{-})$ 1231 cm^{-1} – [*1122 cm^{-1}*]
ν(N-N) 870 - 827 cm^{-1} – [*890 - 863 cm^{-1}*]

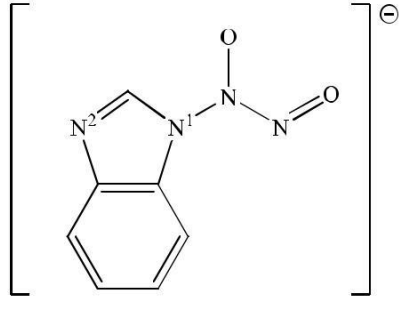

ν_{asym}(O-N-N-O) 1388 cm^{-1} – [*1375 cm^{-1}*]
ν_{sym}(O-N-N-O) 1336 cm^{-1} – [*1346-1321 cm^{-1}*]
$\nu(R_2N^2\text{-}N\text{-})$ 1231 cm^{-1} – [*1228 cm^{-1}*]
ν(N-N) 933 cm^{-1} – [*910 cm^{-1}*]

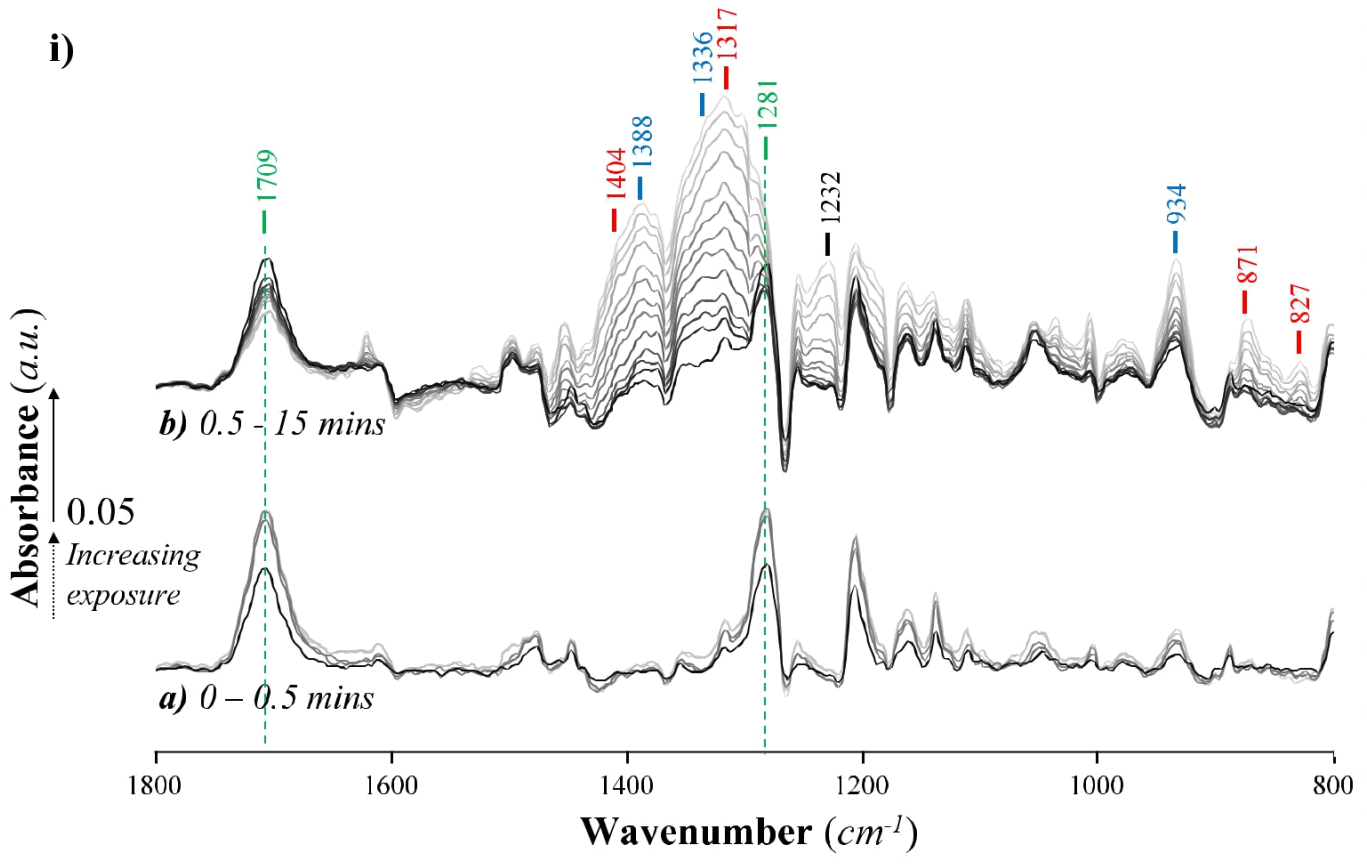

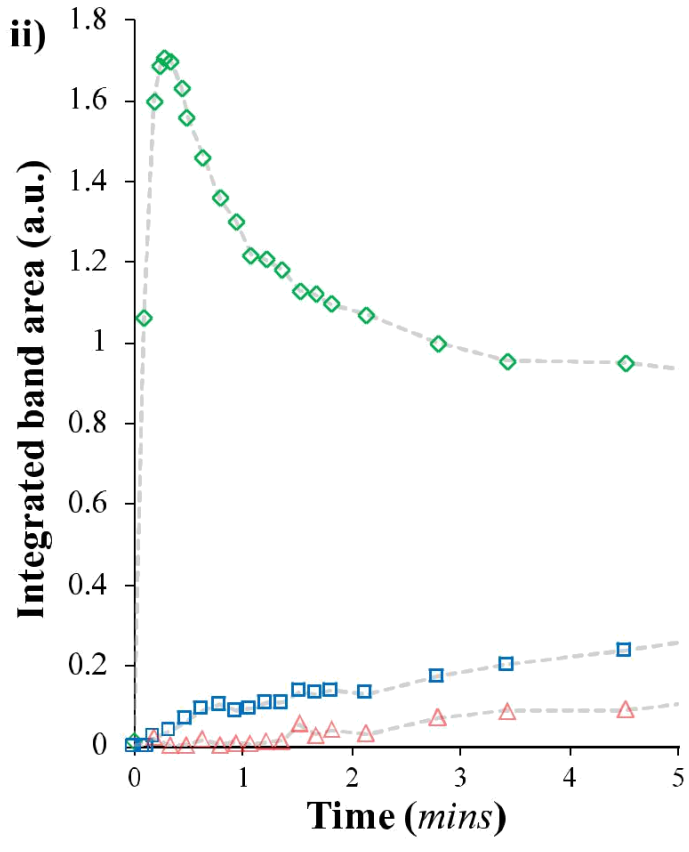

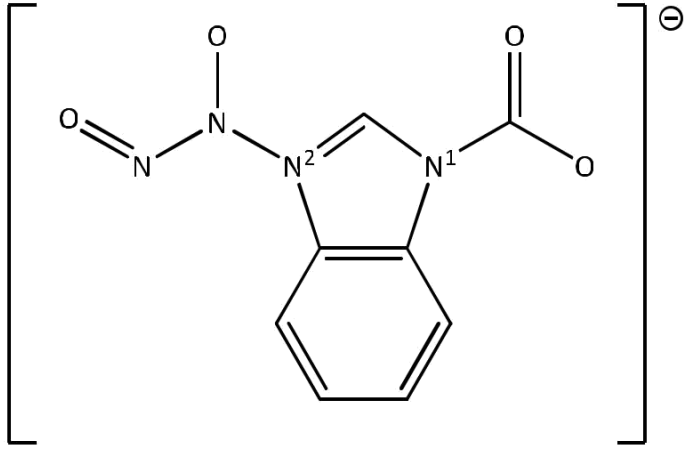

Experimental Bands - [*Calculated bands*]

ν(C=O) 1709 cm^{-1} - [*1844 cm^{-1}*]

$\nu(N^1\text{-}C)$ 1281 cm^{-1} - [*1242 cm^{-1}*]

ν_{asym}(O-N-N-O) 1388 cm^{-1} - [*1459 cm^{-1}*]

ν_{sym}(O-N-N-O) 1336 cm^{-1} - [*1387 cm^{-1}*]

$\nu(R_2N^2\text{-}N)$ 1232 cm^{-1} - [*1242 cm^{-1}*]

ν(N-N) 934 cm^{-1} - [*909 cm^{-1}*]

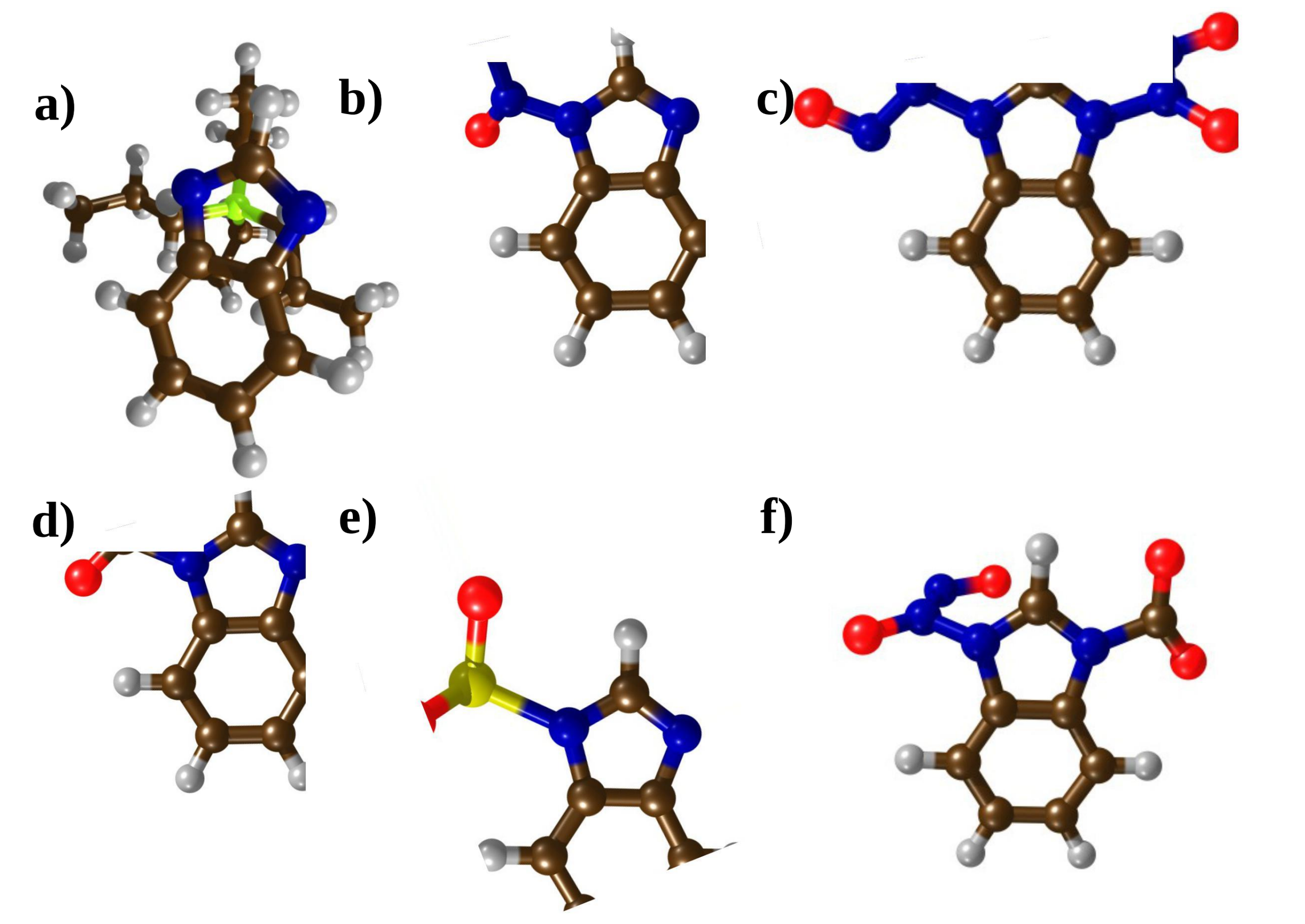
a)
b)
c)
d)
e)
f)

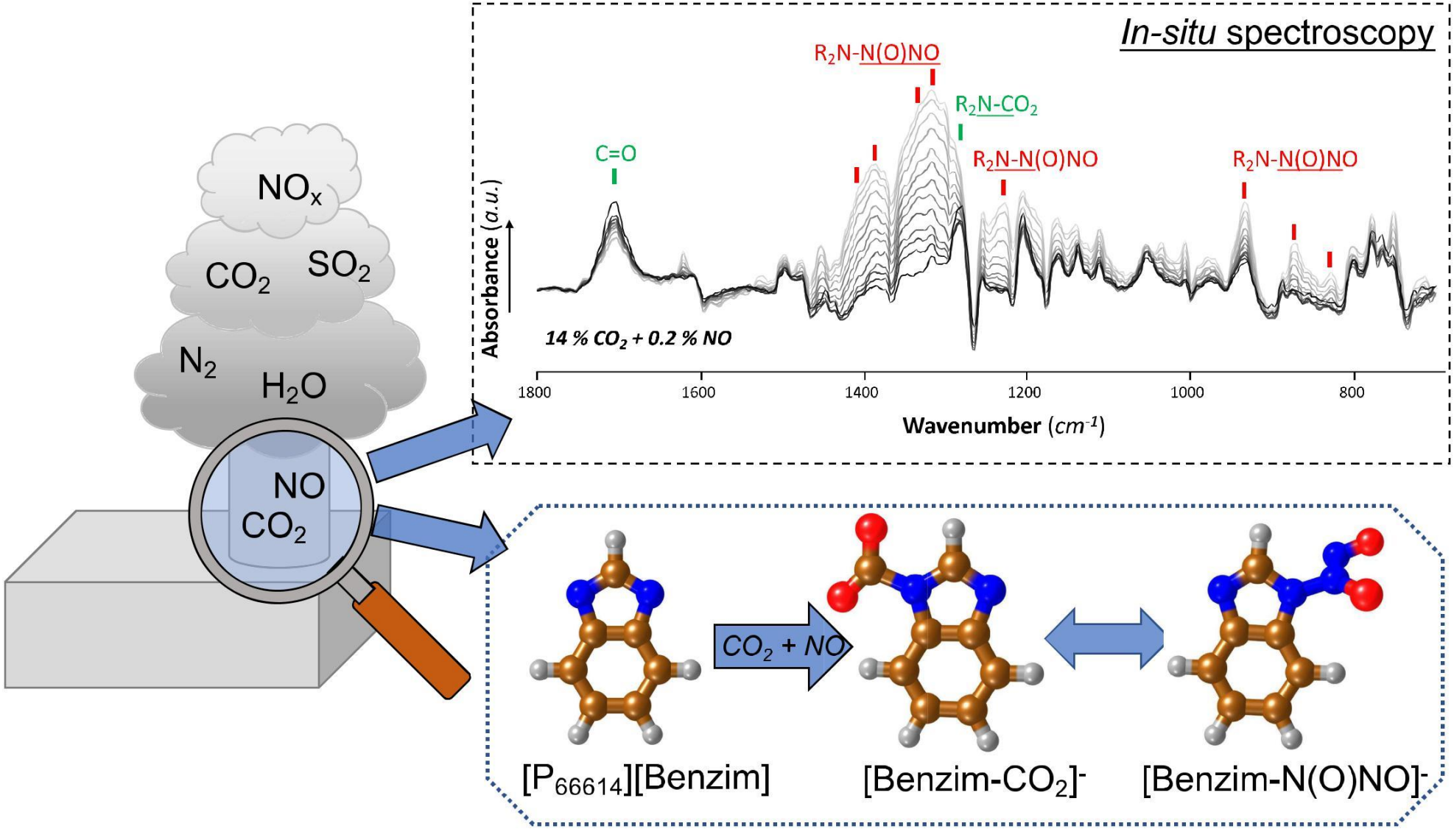
NOx
CO2
SO2
N2
H2O
NO
CO2
In-situ spectroscopy
R2N-N(O)NO
R2N-CO2
C=O
R2N-N(O)NO
R2N-N(O)NO
Absorbance (a.u.)
14 % CO2 + 0.2 % NO
1800
1600
1400
1200
1000
800
Wavenumber (cm-1)
CO2 + NO
[P66614][Benzim]
[Benzim-CO2]-
[Benzim-N(O)NO]-